Sensors and Materials, Vol. 33, No. 6 (2021) 2179–2185
MYU Tokyo

S & M 2605

Scintillation Properties of Dy-doped $50NaPO_3$–$50Al(PO_3)_3$ Glasses

Takayuki Yanagida,[1*] Yutaka Fujimoto,[2] Hirokazu Masai,[3] Go Okada,[4]
Takumi Kato,[1] Daisuke Nakauchi,[1] and Noriaki Kawaguchi[1]

[1]Division of Materials Science, Nara Institute of Science and Technology (NAIST),
8916-5 Takayama, Ikoma, Nara 630-0192, Japan
[2]Department of Applied Chemistry, Graduate School of Engineering, Tohoku University,
6-6-07 Aoba, Aramaki, Aoba-ku, Sendai 980-8579, Japan
[3]National Institute of Advanced Industrial Science and Technology,
1-8-31 Midorigaoka, Ikeda, Osaka 563-8577, Japan
[4]Co-creative Research Center of Industrial Science and Technology (CIST), Kanazawa Institute of Technology,
3-1 Yatsukaho, Hakusan, Ishikawa 924-0838, Japan

(Received January 31, 2021; accepted April 23, 2021)

Keywords: scintillator, glass, TSL, photoluminescence, Dy^{3+}

0.5, 1.0, 5.0, and 10.0 mol% Dy-doped $50NaPO_3$–$50Al(PO_3)_3$ glasses were synthesized by the melt-quenching method. All the samples had a high transmittance of up to 90% at visible wavelengths, and some intense emission lines were observed in their photoluminescence and scintillation spectra. When the glasses were irradiated with X-rays with various doses, a linear relationship between the irradiation dose and the thermally stimulated luminescence intensity was confirmed from 10 to 10000 mGy.

1. Introduction

Ionizing radiation has been utilized for many applications owing to its high penetration power for all materials. To use such ionizing radiation as a useful probe, radiation detectors must be used. Historically, most radiation detectors have been solid-state materials because a high interaction probability with ionizing radiation can be achieved by such materials. Solid-state detectors are mainly classified into two types, semiconductor- and luminescence-type detectors. The former, of which CdTe and TlBr are representatives, can convert the absorbed energy of ionizing radiation to electrons.[1–4] The latter are based on luminescent materials combined with photodetectors, which are used to convert the luminescence to electrons via photoelectric conversion. Luminescent materials for ionizing radiation detectors are mainly divided into scintillators[5] and dosimeter materials.[6] Scintillators can immediately convert the absorbed energy of ionizing radiation to low-energy photons, and dosimeter materials can store the absorbed energy by a form of carrier trapping. Although these two kinds of luminescent materials have been separately discussed in different communities until recently, we proposed an inversely proportional relationship between scintillation intensity and storage luminescence in dosimeter materials based on simple energy conservation.[7,8] Since our proposal, an empirical

*Corresponding author: e-mail: t-yanagida@ms.naist.jp
https://doi.org/10.18494/SAM.2021.3315

ISSN 0914-4935

law that materials with low scintillation intensity are suitable for dosimeters and materials with high scintillation intensity are suitable for scintillators has been confirmed by various experiments.

To detect ionizing radiation efficiently, the use of bulk materials is essential since the probability of an interaction between ionizing radiation and a detector material simply depends on the volume of the material. To satisfy this requirement, bulk single crystals,[9–19] ceramics,[20–31] and glasses[32–38] have been applied for scintillators and dosimeters. Among these material forms, glasses have some advantages such as high chemical durability and high light transmittance, which are preferable for scintillator and dosimeter uses. Although Li-glass scintillators[39–41] and Ag-doped phosphate glasses for radiophotoluminescence dosimeters[42–44] are now commercially available, there remains room for the further study of glass materials.

In the present work, we focus on Dy-doped $50NaPO_3$–$50Al(PO_3)_3$ (hereafter, NAP) glasses in terms of their optical, scintillation, and thermally stimulated luminescence (TSL) dosimetric properties. Previously, our group reported the scintillation and dosimetric properties of NAP glasses doped with all the rare earths except for Pm-doped NAP[45] glasses. Among these glasses, the Tb- and Dy-doped glasses exhibited the highest emission intensity, especially for TSL. Although the Tb concentration dependence of NAP glasses has already been investigated in detail,[46] the Dy concentration dependence of NAP glasses has not yet been examined.

2. Materials and Methods

Sample glasses were prepared by the conventional melt-quenching method. The starting materials were mixed and melted in an alumina crucible inside an electric furnace at 1200 °C for 30 min under ambient atmosphere. The experimental conditions followed those in our previous work.[45] Dy with concentrations of 0.5, 1.0, 5.0, and 10.0 mol% was added to the NAP host. After the synthesis, all the samples were polished to ~ 1 mm thickness, and their transmittance was evaluated using a JASCO V670 spectrometer. Photoluminescence (PL) excitation, an emission contour map, and the PL quantum yield (*QY*) were measured using a Quantaurus-QY spectrometer (Hamamatsu). PL decay times were evaluated using a Quantaurus-τ instrument, where the excitation and monitoring wavelengths were selected from the contour graph. Following optical characterizations, scintillation spectra and decay times were observed under X-ray irradiation using our original setups.[47,48] TSL glow curves and dose responses were evaluated by using a TL2000 (Nanogray) measuring system with a heating rate of 1 °C/s.[49]

3. Results

Figure 1 shows a photograph of the NAP glasses doped with different quantities of Dy under room light. All the glasses were visibly transparent. Figure 2 shows the transmittance spectra of the Dy-doped NAP glasses. All the samples showed ~90% transmittance at visible wavelengths, and some absorption lines due to Dy^{3+} 4f–4f transitions were detected. In Fig. 2, typical electron transitions of each absorption line are shown.[50]

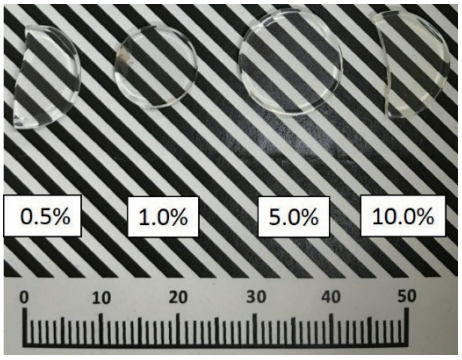

Fig. 1. (Color online) Photograph of Dy-doped NAP glasses after polishing.

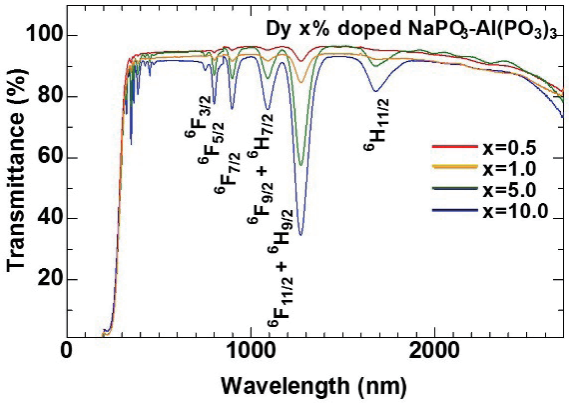

Fig. 2. (Color online) Transmittance spectra of Dy-doped NAP glasses.

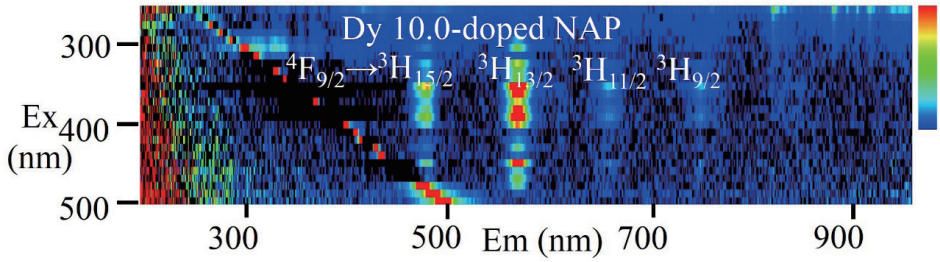

Fig. 3. (Color online) PL emission (horizontal axis) and excitation (vertical axis) contour graph of 10.0% Dy-doped NAP glass.

Figure 3 shows the PL emission and excitation contour graph of 10.0% Dy-doped NAP glass as a representative example. Intense emission lines at 480, 570, 660, and 750 nm due to the electron transitions of $^4F_{9/2}$ -> $^3H_{15/2}$, $^3H_{13/2}$, $^3H_{11/2}$, and $^3H_{9/2}$, respectively,[50] were detected upon 300–500 nm excitation. The PL *QY* of the Dy-doped NAP glasses as a function of Dy concentration is shown in Fig. 4. Here, the PL *QY*s were calculated by summing the emission intensities of the four above-mentioned emission lines upon 390 nm excitation, with previous data[45] for a 0.3% Dy-doped NAP glass also shown. The glass doped with 0.5% Dy exhibited the highest PL *QY* . Figure 5 presents PL decay curves of the Dy-doped NAP glasses monitored at 570 nm upon 390 nm excitation. All the decay curves revealed faster and slower components. The faster component was considered to originate from the excitation pulse, and the slower one was considered to originate from the Dy^{3+} $^4F_{9/2}$ -> $^3H_{13/2}$ transition. To deduce the PL decay times due to emissions from Dy^{3+}, the tail part of the curves was approximated by a single exponential function. The decay times of the NAP glasses doped with 0.5, 1.0, 5.0, and 10.0% Dy were found to be 893, 775, 361, and 234 μs, respectively. Concentration quenching was observed in the NAP glasses doped with the highest concentrations of Dy (5.0 and 10.0%).

Figure 6 shows the X-ray-induced scintillation spectra of the Dy-doped NAP glasses. Three intense emission lines were detected at 480, 570, and 660 nm originating from 4f–4f transitions

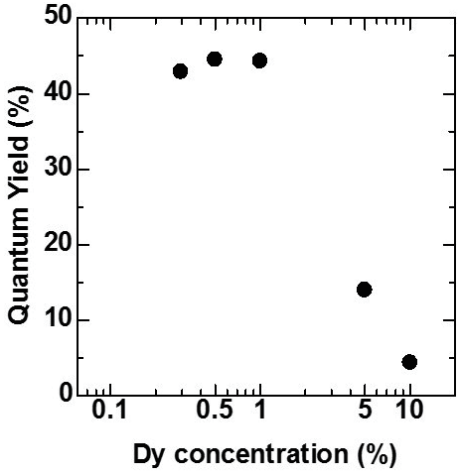

Fig. 4. PL *QY* of Dy-doped NAP glasses as a function of Dy concentration.

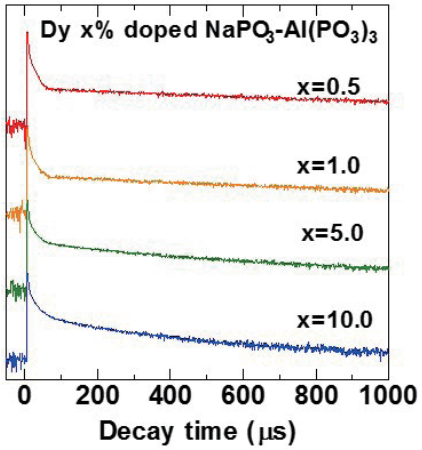

Fig. 5. (Color online) PL decay curves of Dy-doped NAP glasses upon 390 nm excitation monitored at 570 nm.

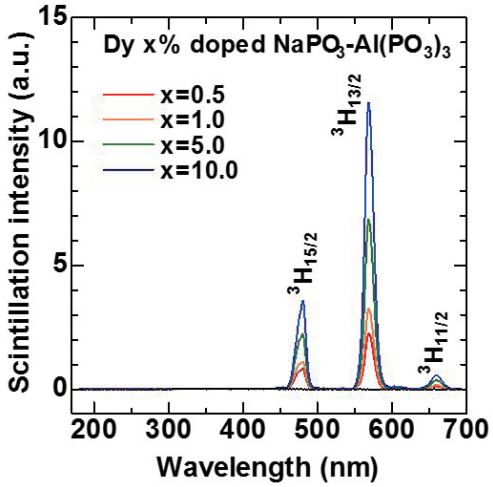

Fig. 6. (Color online) X-ray-induced scintillation spectra of Dy-doped NAP glasses.

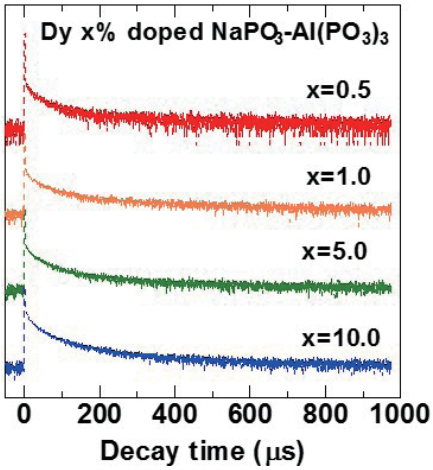

Fig. 7. (Color online) X-ray-induced scintillation decay curves of Dy-doped NAP glasses.

of Dy^{3+}. Owing to the limited wavelength sensitivity of our instrument, no emission longer than 700 nm was observed. In spite of the 5.0% Dy-doped NAP glass being the largest sample, the 10.0% Dy-doped NAP glass exhibited the highest scintillation intensity. Figure 7 shows scintillation decay curves of the Dy-doped NAP glasses under X-ray irradiation. These decay curves were analyzed in the same manner as the PL decay curves, and the scintillation decay times of the NAP glasses doped with 0.5, 1.0, 5.0, and 10.0% Dy were found to be 448, 329, 156, and 92 μs, respectively. The scintillation decay times were shorter than the PL decay times, and in such a case, quenching via an interaction among excited electrons (secondary electrons) will occur.

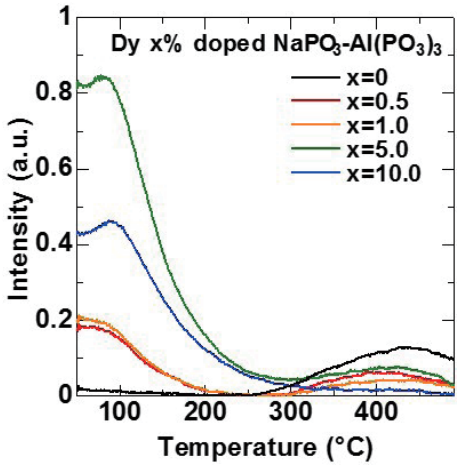

Fig. 8. (Color online) TSL glow curves of Dy-doped NAP glasses after 1 Gy X-ray irradiation.

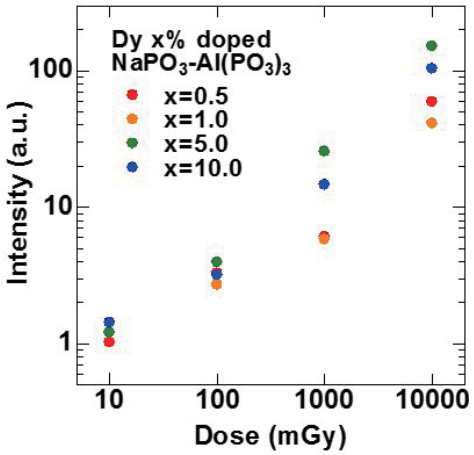

Fig. 9. (Color online) Dose responses of Dy-doped NAP glasses.

Figure 8 shows TSL glow curves of the Dy-doped NAP glasses after 1 Gy X-ray irradiation. Here, in order to consider the origin of the TSL, data of the undoped NAP glass is also plotted. Broad glow peaks were observed at ~100 and ~400 °C in the Dy-doped samples while the undoped sample showed only the ~400 °C peak. From this comparison of Dy-doped and undoped NAP, the glow peak at ~100 °C was generated by Dy doping, and the origin of the ~400 °C peak was attributed to the NAP host. The Dy concentration dependence of the TSL intensity was different from those of the transmittance and scintillation intensities. One possible reason is fading due to the ~90 °C peak. In the measurements, we moved samples from where they were subjected to X-ray irradiation to the setup for TSL measurement as soon as possible after the irradiation. However, an equal fading condition for each sample could not be achieved. The main discrepancy was between the 5.0- and 10.0%-doped samples, and the complementary relationship[8] between scintillation and storage luminescence may have also contributed to the different Dy concentration dependences of the TSL intensity. Figure 9 depicts the X-ray dose responses of the Dy-doped NAP glasses. Among the present samples, the NAP glasses doped with 5.0 and 10.0% Dy showed better performance than the other doped glasses, and a linear response from 10 to 10000 mGy was confirmed.

4. Conclusions

NAP glasses doped with 0.5, 1.0, 5.0, and 10.0% Dy were fabricated by the melt-quenching method. All the samples were visibly transparent, and the maximum PL *QY* was ~45% for the 0.5% Dy-doped sample. Intense emission lines at 480, 570, and 660 nm were detected in both the PL and scintillation spectra, and their decay times were several hundred ms. Two intense glow peaks were detected at ~100 and ~400 °C in the TSL glow curves of the samples. The origins of the ~100 and ~400 °C peaks were attributed to the introduction of Dy ions and the NAP host, respectively.

Acknowledgments

This work was supported by the Cooperative Research Project of Research Center for Biomedical Engineering, Nippon Sheet Glass Foundation, and Japan Society for the Promotion of Science (JSPS) through Grants-in-Aid for Scientific Research B (19H03533).

References

1 V. M. Sklyarchuk, V. A. Gnatyuk, and T. Aoki: Nucl. Instrum. Methods Phys. Res., Sect. A **953** (2020) 163224.
2 M. Koshimizu, Y. Muroya, S. Yamashita, M. Nogami, K. Hitomi, Y. Fujimoto, and K. Asai: Sens. Mater. **32** (2020) 1445.
3 K. Watanabe, K. Matsumoto, A. Unitani, K. Hitomi, M. Nogami, and W. Kockelmann: Sens. Mater. **32** (2020) 1435.
4 V. M. Sklyarchuk, V. A. Gnatyuk, and T. Aoki: IEEE Trans. Nucl. Sci. **66** (2019) 2140.
5 T. Yanagida: Proc. Japan Academy, B **94** (2018) 75.
6 T. Yanagida, G. Okada, and N. Kawaguchi: J. Lumin. **207** (2019) 14.
7 T. Yanagida, Y. Fujimoto, K. Watanabe, K. Fukuda, N. Kawaguchi, Y. Miyamoto, and H. Nanto: Rad. Meas. **71** (2014) 162.
8 T. Yanagida: J. Lumin. **169** (2016) 544.
9 Y. Fujimoto, K. Saeki, D. Nakauchi, T. Yanagida, M. Koshimizu, and K. Asai: Sens. Mater. **31** (2019) 1248.
10 T. Abe, Y. Suzuki, A. Nakagawa, T. Chiba, M. Nakagawa, Y. Kashiwaba, I. Niikura, Y. Kashiwaba, and H. Osada: J. Mater. Sci.: Mater. Electron. **30** (2019) 16873.
11 P. Kantuptim, M. Akatsuka, D. Nakauchi, T. Kato, N. Kawaguchi, and T. Yanagida: Sens. Mater. **32** (2020) 1357.
12 D. N. Krishnakumar and R. N. Perumal: J. Mater. Sci.: Mater. Electron. **31** (2020) 4294.
13 M. Akatsuka, D. Nakauchi, T. Kato, N. Kawaguchi, and T. Yanagida: Sens. Mater. **32** (2020) 1373.
14 I. Adell, M. C. Pujol, R. M. Solé, M. Aguiló, and F. Díaz: J. Lumin. **225** (2020) 117339.
15 D. Nakauchi, T. Kato, N. Kawaguchi, and T. Yanagida: Sens. Mater. **32** (2020) 1389.
16 F. Chiossi, S. Vasiukov, A. F. Borghesani, C. Braggio, A. Di Lieto, M. Tonelli, and G. Carugno: J. Lumin. **219** (2020) 116883.
17 Y. Takebuchi, H. Fukushima, T. Kato, D. Nakauchi, N. Kawaguchi, and T. Yanagida: Sens. Mater. **32** (2020) 1405.
18 N. Matsubayashi, H. Tanaka, T. Takata, K. Okazaki, Y. Sakurai, and M. Suzuki: Radiat. Meas. **140** (2021) 106489.
19 T. Yanagida, M. Sakairi, T. Kato, D. Nakauchi, and N. Kawaguchi: Appl. Phys. Exp. **13** (2020) 016001.
20 P. R. González, O. Ávila, D. Mendoza-Anaya, L. Escobar-Alarcón, and A. González-Romero: J. Mater. Sci.: Mater. Electron. **31** (2020) 12191
21 H. Kimura, T. Kato, D. Nakauchi, M. Koshimizu, N. Kawaguchi, and T. Yanagida: Sens. Mater. **31** (2019) 1265.
22 K. V. Ivanovskikh, V. A. Pustovarov, S. Omelkov, M. Kirm, F. Piccinelli, and M. Bettinellic: J. Lumin. **230** (2021) 117749.
23 H. Kimura, T. Kato, D. Nakauchi, N. Kawaguchi, and T. Yanagida: Sens. Mater. **32** (2020) 1381.
24 Y. Shi, Y. Zhao, M. Cao, H. Chen, Z. Hu, X. Chen, Z. Zhan, and Q. Liu: J. Lumin. **225** (2020) 117336.
25 T. Kato, D. Nakauchi, N. Kawaguchi, and T. Yanagida: Sens. Mater. **32** (2020) 1411.
26 P. Bilski, B. Obryk, W. Gieszczyk, and P. Baran: Radiat. Meas. **139** (2020) 106486.
27 N. Kawaguchi, G. Okada, Y. Futami, D. Nakauchi, T. Kato, and T. Yanagida: Sens. Mater. **32** (2020) 1419.
28 A. Ulanowski, M. Hiller, and C. Woda: Radiat. Meas. **140** (2021) 106458.
29 D. Maruyama, S. Yanagisawa, Y. Koba, T. Andou, and K. Shinsho: Sens. Mater. **32** (2020) 1461.
30 E. G. Yukihara: Radiat. Meas. **134** (2020) 106291.
31 S. Yanagisawa, D. Maruyama, R. Oh, Y. Koba, T. Andoh, and K. Shinsho: Sens. Mater. **32** (2020) 1479.
32 N. Kawaguchi and T. Yanagida: Sens. Mater. **31** (2019) 1257.
33 M. W. Kielty, L. Pan, M. A. Dettmann, V. Herrig, U. Akgun, and L. G. Jacobsohn: J. Mater. Sci.: Mater. Electron. **30** (2019) 16774.
34 D. Shiratori, Y. Isokawa, N. Kawaguchi, and T. Yanagida: Sens. Mater. **31** (2019) 1281.
35 H. M. Diab, A. M. Abdelghany, and H. S. Hafez: J. Mater. Sci.: Mater. Electron. **31** (2020) 20452.

36 D. Shiratori, D. Nakauchi, T. Kato, N. Kawaguchi, and T. Yanagida: Sens. Mater. **32** (2020) 1365.
37 V. Bhatia, D. Kumar, A. Kumar, V. Mehta, S. Chopra, A. Vij, S. M. D. Rao, and S. P. Singh: J. Mater. Sci.: Mater. Electron. **30** (2019) 677.
38 A. Ishikawa, A. Yamazaki, K. Watanabe, S. Yoshihashi, A. Uritani, Y. Sakurai, H. Tanaka, R. Ogawara, M. Suda, and T. Hamano: Sens. Mater. **32** (2020) 1489.
39 F. W. K. Firk, G. G. Slaughter, and R. J. Ginther: Nucl. Instrum. Methods **13** (1961) 313.
40 S. Sakamoto: Nucl. Instrum. Methods Phys. Res., Sect. A **299** (1990) 182.
41 J. Pausch, F. Scherwinski, and J. Stein: Nucl. Instrum. Methods Phys. Res., Sect. A **807** (2016) 121.
42 F. d'Errico, L. Abegão, S. O. Souza, A. Chierici, L. Lazzeri, M. Puccini, S. Vitoloa, Y. Miyamoto, H. Nanto, and T. Yamamoto, Rad. Meas. **137** (2020) 106423.
43 T. Yamamoto, Y.Yanagida-Miyamoto, T. Iida, and H. Nanto: Rad. Meas. **136** (2020) 106363.
44 T. Kurobori, W. Kada, Y. Yanagida, Y. Koguchi, and H. Nanto: Rad. Meas. **140** (2021) 106473.
45 T. Kuro, G. Okada, N. Kawaguchi, Y. Fujimoto, H. Masai, and T. Yanagida: Opt. Mater. **62** (2016) 561.
46 N. Kawano, M. Akatsuka, H. Kimura, G. Okada, N. Kawaguchi, and T. Yanagida: Radiat. Meas. **117** (2018) 52.
47 T. Yanagida, K. Kamada, Y. Fujimoto, H. Yagi, and T. Yanagitani: Opt. Mater. **35** (2013) 2480.
48 T. Yanagida, Y. Fujimoto, T. Ito, K. Uchiyama, and K. Mori: Appl. Phys. Exp. **7** (2014) 062401.
49 T. Yanagida, Y. Fujimoto, N. Kawaguchi, and S. Yanagida: J. Ceram. Soc. Jpn. **121** (2013) 988.
50 M. E. Alvarez-Ramos: J. Lumin. **233** (2021) 117874.